



# Supplementary Materials: Clinically expired platelet concentrates as a source of extracellular vesicles for targeted anti-cancer drug delivery

Ana Meliciano <sup>1,2,†</sup>, Daniela Salvador <sup>1,2,†</sup>, Pedro Mendonça <sup>3</sup>, Ana Filipa Louro <sup>1,2</sup>, Margarida Serra <sup>1,2,\*</sup>

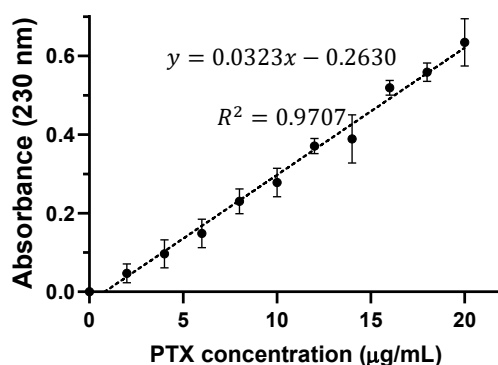
<sup>1</sup> iBET, Instituto de Biologia Experimental e Tecnológica, Apartado 12, 2781-901 Oeiras, Portugal.

<sup>2</sup> ITQB-NOVA, Instituto de Tecnologia Química e Biológica António Xavier, Universidade Nova de Lisboa, Avenida da República, 2780-157 Oeiras, Portugal.

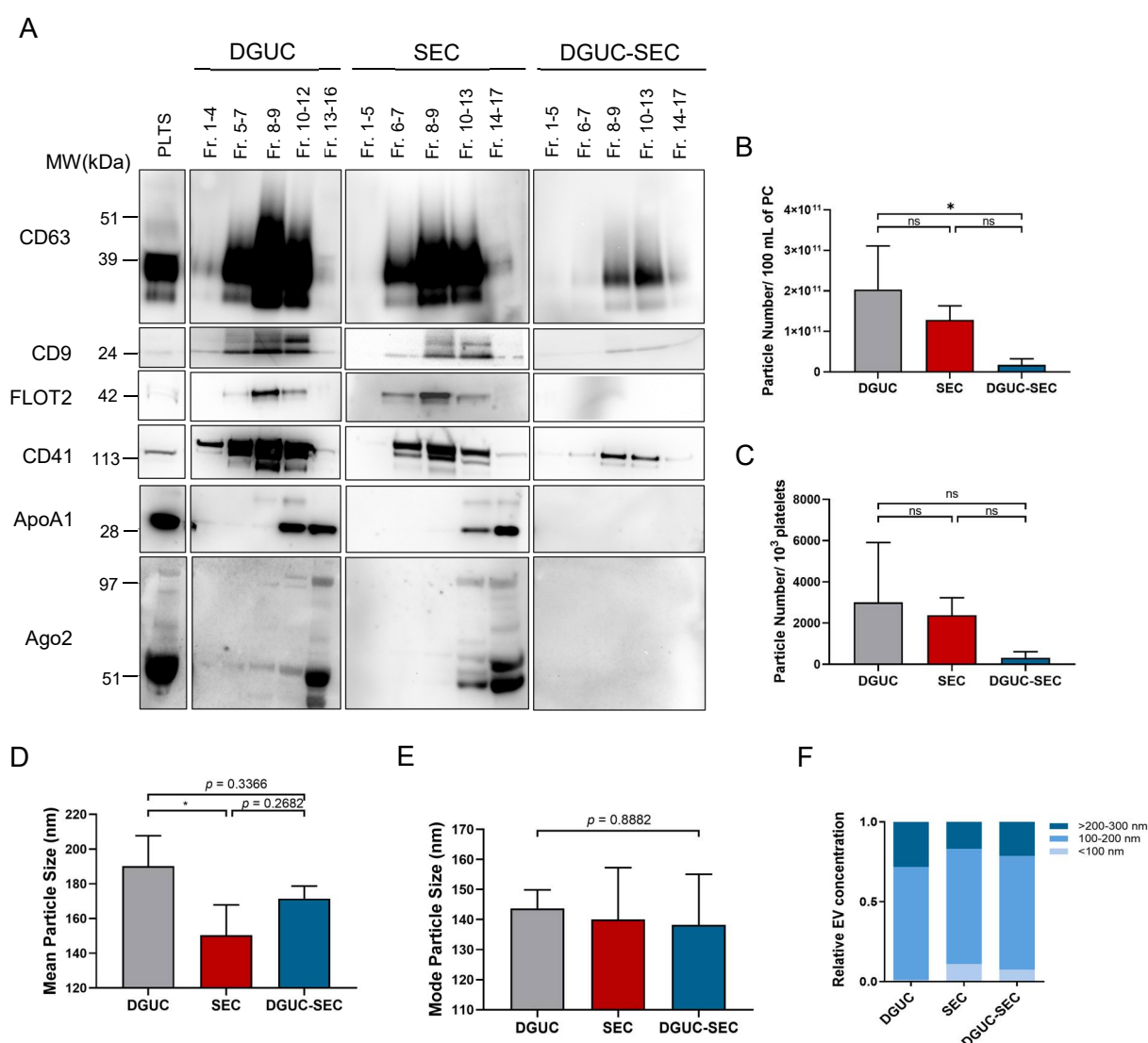
<sup>3</sup> IPST, Instituto Português do Sangue e da Transplantação, 1740-005 Lisboa, Portugal.

\* Correspondence: mserra@ibet.pt

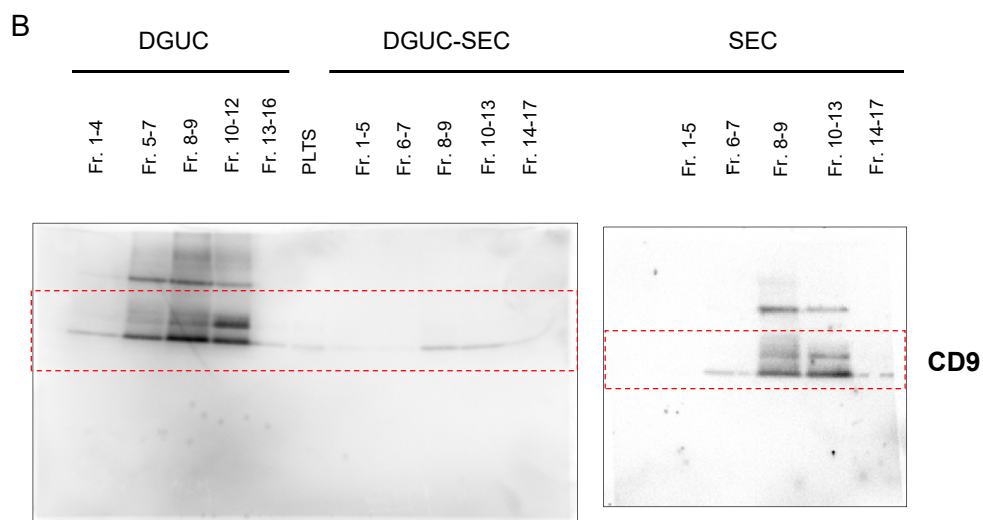
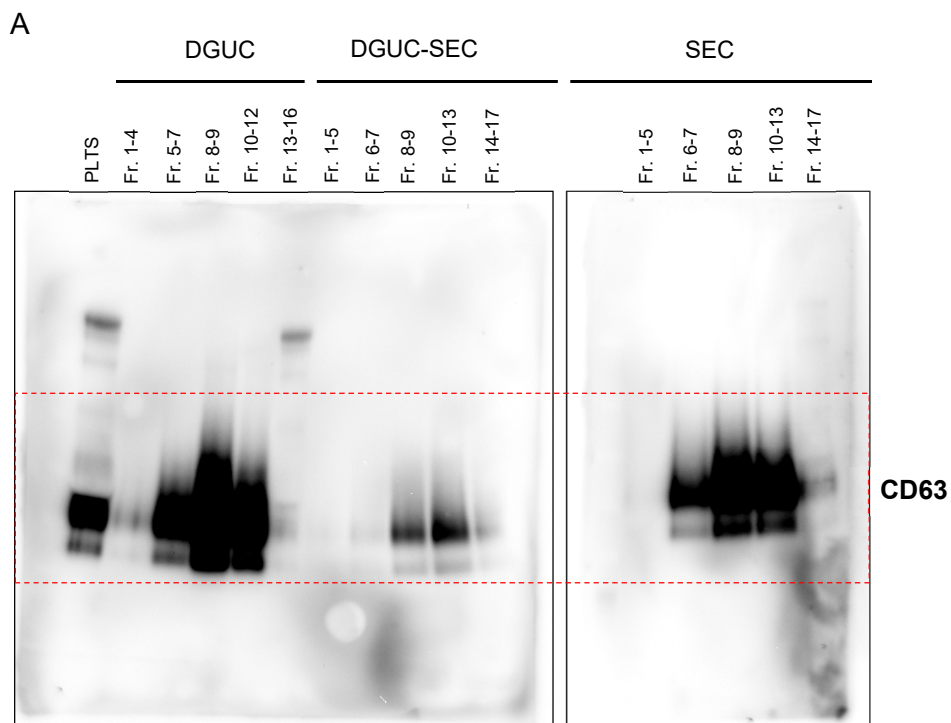
† These authors contributed equally to this work.

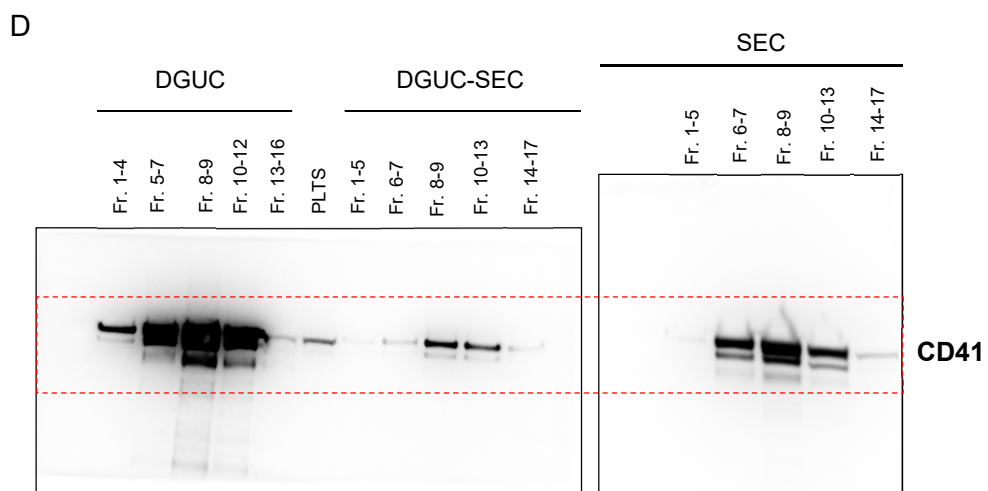
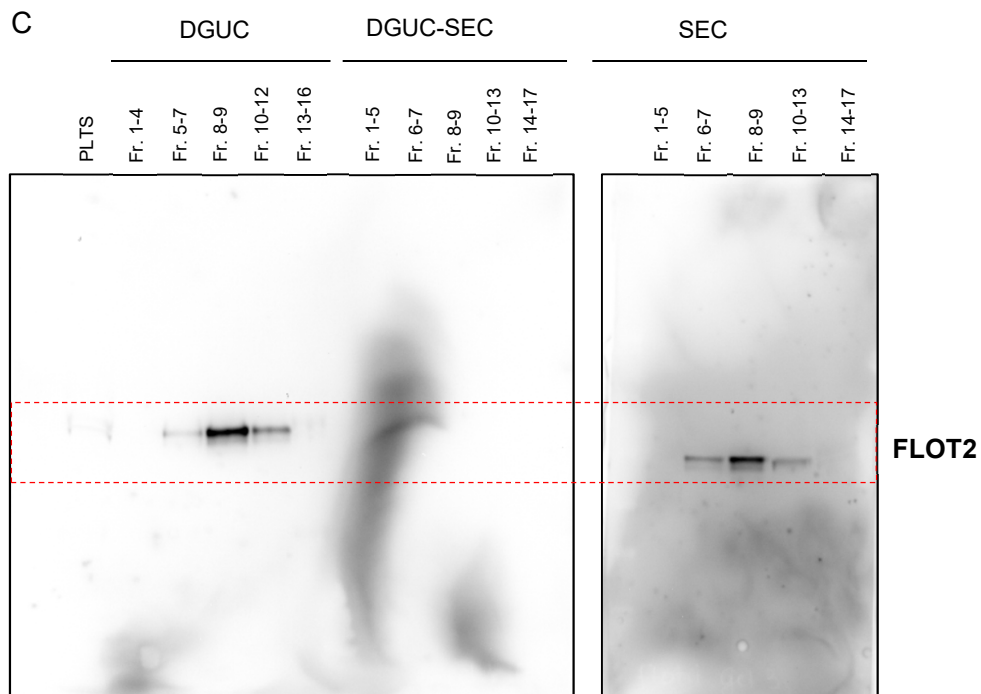


**Figure S1.** Paclitaxel calibration curve used to estimate PTX concentration into pEV.  $n=3$ ,  $n$  represents independent experiments carried out inter-days.



**Figure S2.** Characterization of pEV fractions isolated by DGUC, SEC, and DGUC-SEC in terms of purity, yield, and size distribution. **(A)** Western Blot analysis of specific EV markers (tetraspanins CD63 (glycosylated form) and CD9, and cytosolic protein flotillin-2), platelet-specific marker (CD41), and non-EV markers [apolipoprotein (ApoA1) and argonaute 2 (Ago2)] in pooled fractions and platelet lysate (PLTS). Molecular weight markers (MW, KDa) are indicated. **(B)** pEV-enriched fractions (Fr.8-9) were analyzed using nanoparticle tracking analysis. Particle number was normalized to platelet concentrate (PC) volume (100 mL) and **(C)** platelet count ( $10^3$  platelets); ( $n=3$ ). **(D)** Mean and **(E)** mode particle size (nm) of pEV samples; ( $n=3$ ). **(F)** Relative pEV distribution ranged into three different size classes: < 100 nm, 100-200 nm and >200-300 nm; ( $n=3$ ).  $n$  represents biologically independent replicates. Data are represented as mean  $\pm$  S.D. \* $p < 0.05$ , n.s. not significant, determined by one-way ANOVA followed by Tukey's multiple comparison test.





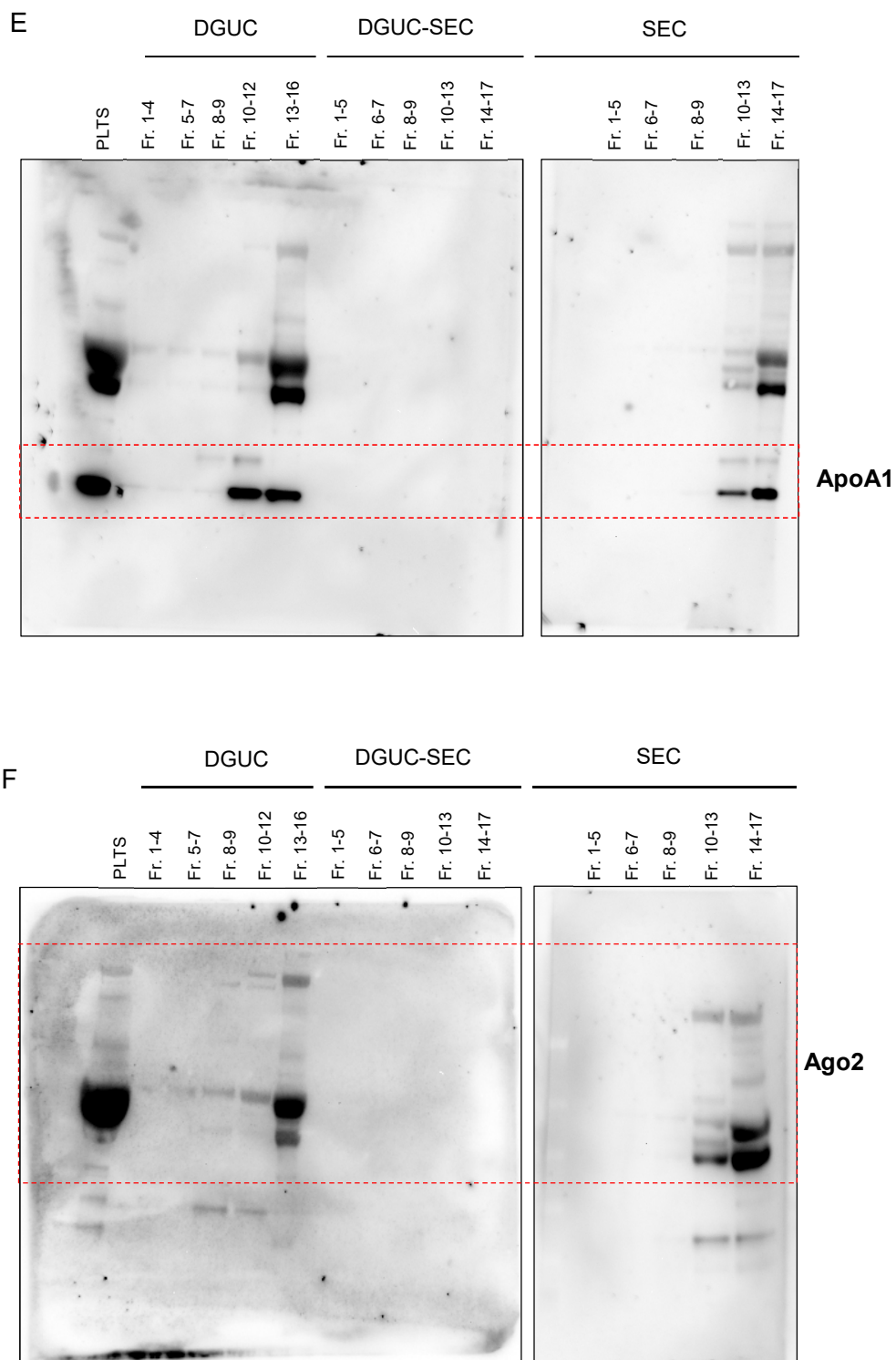


**Figure S3.** Full-length western blotting images for the results shown in main figures and supplementary Figure S2. Insets indicate cropped regions.

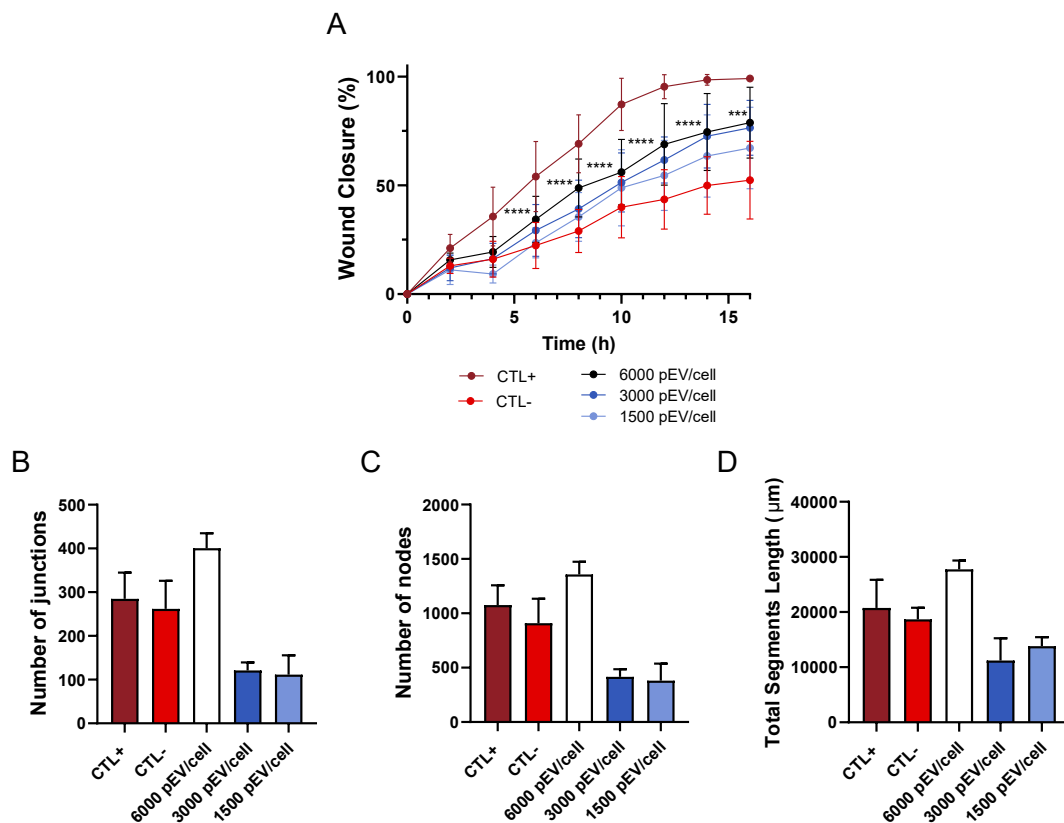


**Figure S4.** Effect of different pEV densities on HUVEC angiogenesis. **(A)** Quantitative analysis of the wound closure percentage throughout culture time. HUVEC were treated with 1500, 3000 and 6000 pEV/cell or with controls, CTL+ (cells cultured in supplemented media) and CTL- (8-9 fractions of DPBS gradient), for 16 h; ( $n=3$ ). **(B)** Number of junctions, **(C)** nodes and **(D)** total segments length ( $\mu\text{m}$ ) of HUVEC incubated with pEV or with controls, CTL+ and CTL-, for 8 h. Data are represented as mean  $\pm$  S.D. One-way ANOVA followed by Tukey's multiple comparison test (6000 pEV/cell versus CTL-). \*\*\* $p < 0.001$ , \*\*\*\* $p < 0.0001$ .

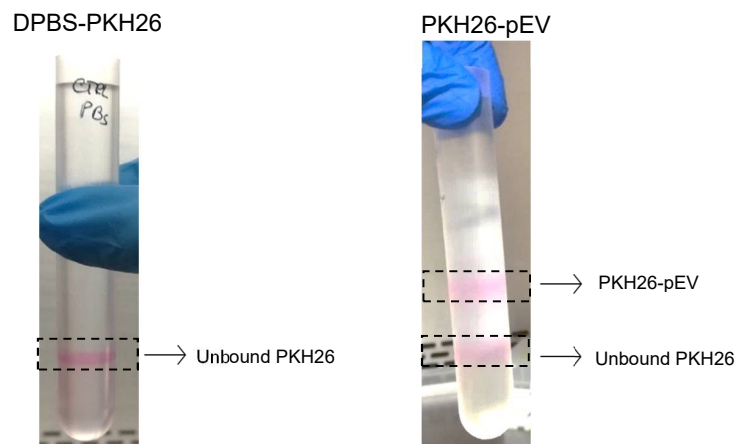


**Figure S5.** Separation of PKH26-pEV by DGUC. The presence of the two bands marked in the figure indicates a clear separation of PKH26-pEV (upper band) at the level of fractions enriched in pEV (fractions 8 and 9) from the unbound dye (lower band) located in denser fractions.

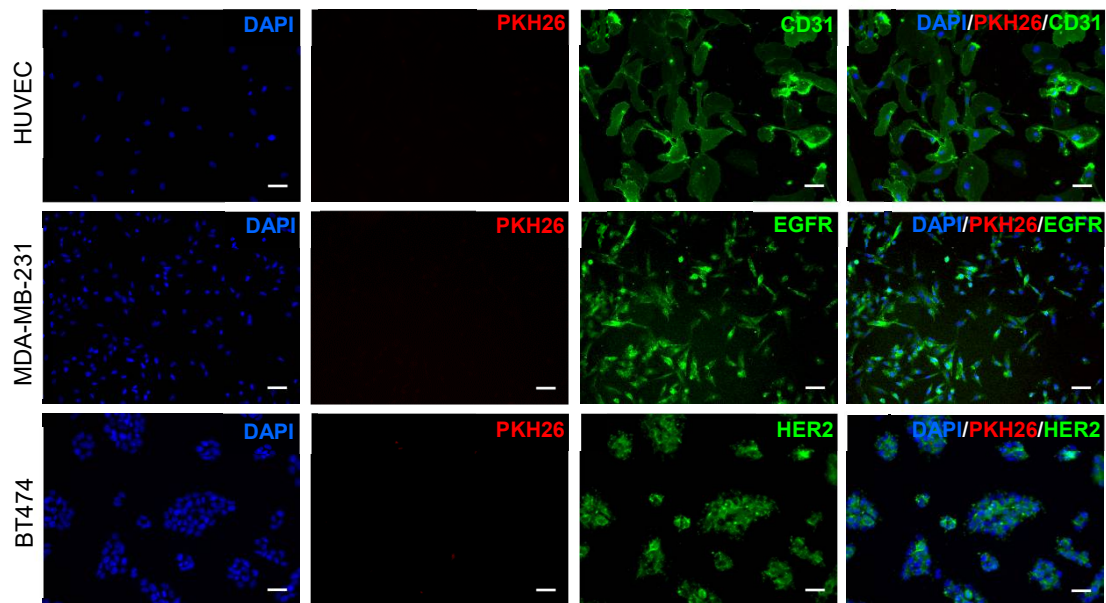


**Figure S6.** Cellular uptake of DPBS-PKH26 (negative control) by HUVEC, MDA-MB-231, and BT474 cells after 24 h of incubation. Representative immunofluorescence images of DPBS-PKH26 treatment. HUVEC, MDA-MB-231, and BT474 cells were stained for CD31, EGFR, and HER2 (green), respectively, and nuclei (DAPI, blue). Scale bars: 50  $\mu\text{m}$ .

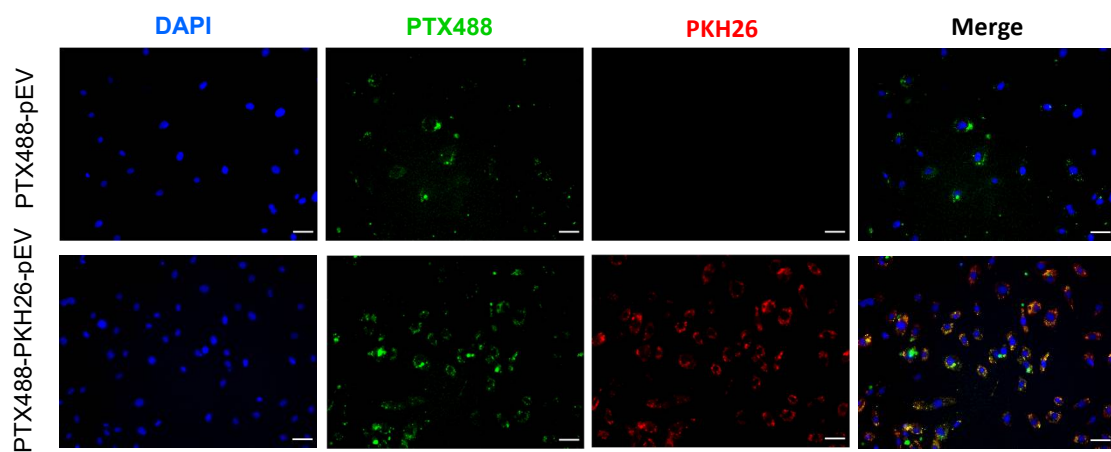


**Figure S7.** Intracellular distribution of PTX-loaded pEV in HUVEC cells after 24 h of incubation. HUVEC were treated with pEV loaded with tagged PTX (PTX488, green) and PTX488-pEV labeled with PKH26 (red) (PTX488-PKH26-pEV). Cell nuclei were stained with DAPI (blue), and cells were analyzed by fluorescence microscopy. Scale bars: 50  $\mu\text{m}$ .